university of groningen

University Medical Center Groningen

University of Groningen

Dynamic optimization of a dead-end filtration trajectory

Blankert, Bastiaan; Kattenbelt, Carolien; Betlem, Ben H.L.; Roffel, Brian

Published in:
Journal of Membrane Science

DOI:
10.1016/j.memsci.2006.12.024

IMPORTANT NOTE: You are advised to consult the publisher's version (publisher's PDF) if you wish to cite from it. Please check the document version below.

Document Version
Publisher's PDF, also known as Version of record

Publication date:
2007

Link to publication in University of Groningen/UMCG research database

Citation for published version (APA):
Blankert, B., Kattenbelt, C., Betlem, B. H. L., & Roffel, B. (2007). Dynamic optimization of a dead-end filtration trajectory: Non-ideal cake filtration. *Journal of Membrane Science*, *290*(1), 114-124. https://doi.org/10.1016/j.memsci.2006.12.024

Copyright
Other than for strictly personal use, it is not permitted to download or to forward/distribute the text or part of it without the consent of the author(s) and/or copyright holder(s), unless the work is under an open content license (like Creative Commons).

The publication may also be distributed here under the terms of Article 25fa of the Dutch Copyright Act, indicated by the “Taverne” license. More information can be found on the University of Groningen website: https://www.rug.nl/library/open-access/self-archiving-pure/taverne-amendment.

Take-down policy
If you believe that this document breaches copyright please contact us providing details, and we will remove access to the work immediately and investigate your claim.

Downloaded from the University of Groningen/UMCG research database (Pure): http://www.rug.nl/research/portal. For technical reasons the number of authors shown on this cover page is limited to 10 maximum.

Download date: 06-05-2023

Available online at www.sciencedirect.com
ScienceDirect
Journal of Membrane Science 290 (2007) 114–124
journal of MEMBRANE SCIENCE
www.elsevier.com/locate/memsci

Dynamic optimization of a dead-end filtration trajectory: Non-ideal cake filtration

Bastiaan Blankert*, Carolien Kattenbelt, Ben H.L. Betlem, Brian Roffel

Faculty of Science and Technology, University of Twente, P.O. Box 217, 7500AE Enschede, The Netherlands

Received 7 March 2006; received in revised form 14 November 2006; accepted 12 December 2006
Available online 22 December 2006

Abstract

A control strategy aimed at minimizing energy consumption is formulated for non-ideal dead-end cake filtration with an inside-out hollow fiber ultrafiltration membrane system. The non-ideal behavior was assumed to originate from cake compression, non-linear cake resistance and a variable pump efficiency.

Constant gross power, constant flux and constant pressure filtration were considered as alternatives for the optimal operating strategy. It was found that the ratio between the initial and final total resistance determines whether a large difference between these strategies occurs. This is mainly determined by the specific cake resistance, the final state and the membrane resistance.

When there is a large difference between the operating strategies, the pump characteristics determine which suboptimal strategies are attractive. For a pump with a low head and a large capacity, constant flux filtration is nearly optimal, whereas for a pump with a large head and a small capacity optimal operation is closer to constant pressure filtration. Under the investigated conditions there was no significant difference (<0.5%) between the constant gross power and the optimal operating strategy.
© 2006 Elsevier B.V. All rights reserved.

Keywords: Dynamic optimization; Cake filtration; Pump efficiency

1. Introduction

Dead-end membrane filtration can be used as a part of a conventional water treatment process or as a stand alone treatment. Due to its high selectivity, it is a promising technology. However, as a consequence of the accumulation of retained matter, filtration becomes progressively more difficult. This is an important limiting factor in the application of membrane filtration systems [1]. Fouling has a direct impact on the operating costs, because a large part of the energy consumption is needed to overcome the fouling resistance. Furthermore, periodic cleaning is necessary. Hence, in the operation of dead-end membrane filtration, fouling can be considered one of the main limitations.

It is believed that the costs associated with membrane fouling are strongly dependent on the operating conditions. Currently these conditions are often based on rules of thumb or pilot plant studies. Hence, optimization may lead to a reduction in operating costs.

Mathematical optimization of membrane operation minimizes the operating costs calculated by a process model. Although filtration models are widely available, to the authors knowledge little has been published about mathematical optimization of membrane filtration. Steady state optimization or momentary optimization deals with finding the optimal value of a certain control variable at a certain moment. For example, in constant pressure filtration the net flow rate can be maximized. This has been applied to a a discontinuous microfiltration-backwash process [2] or a crossflow microfiltration process [3]. However, in industrial applications the flow rate is often a control variable. In that case maximizing the flow rate is not a good objective and the operating costs should be minimized instead. Noronha et al. [4] determined the optimal steady state operating point for a two stage nanofiltration system. The pump efficiency as function of the flow was an important factor in the operating costs.

Dynamic optimization deals with finding the optimal trajectory of a certain state or control variable. This type of

* Corresponding author. Tel.: +31 53 489 2896; fax: +31 53 489 3849.
E-mail address: B.Blankert@utwente.nl (B. Blankert).

0376-7388/$ – see front matter © 2006 Elsevier B.V. All rights reserved.
doi:10.1016/j.memsci.2006.12.024

optimization considers the difficulty of the operation during the entire production phase. This was applied to reverse osmosis filtration of cheese whey by van Boxtel et al. [5]. The result of dynamic optimization can often be interpreted as an operating strategy or an optimal control mode. Currently, well known operating strategies for both a crossflow and dead-end configuration are constant flux and constant pressure filtration.

In the crossflow filtration of raw cane sugar remelt, for example, it was found that the control mode is of importance for the fouling rate [6]. The author suggests that by applying constant flux filtration, the system can be operated under low fouling conditions. This affected microfiltration more strongly than for ultrafiltration. Another example is the crossflow microfiltration of lactic acid fermentation broth [7,8]. Although constant flux filtration allowed for operation under low fouling conditions, the author finds that the average productivity is higher for constant pressure filtration.

In the field of dead-end filtration, constant flux and constant pressure are the most common operating strategies as well. Compared to constant pressure filtration, constant flux filtration is convenenient in industrial application due to its constant production rate. Furthermore, the initial rapid fouling that can occur due to a high initial flux in constant pressure filtration is avoided [9]. However, regarding cake filtration it was found that the operating mode is of less importance on the fouling behavior [10]. The disadvantage of constant flux filtration is the rise of the transmembrane pressure, which can be large under certain conditions.

In this research, the effect of the operating strategy on the operating costs is considered. For dead end filtration, it was found that under the assumptions of the ideal blocking laws, a reduction in energy consumption is possible by applying constant power filtration [11]. Compared to constant flux and constant pressure filtration the reduction in energy consumption is usually small, except in cases where the fouling mechanism resembles standard blocking and the fouling resistance is large. However, this control strategy does not take the effect of pump efficiency, cake compressibility and area reduction in a hollow fiber, into account. Based on the results obtained from the ideal blocking laws it can be expected that constant gross power is a good suboptimal operating strategy. The effect of a variable pump efficiency, cake volume and cake compressibility on the optimal strategy and the reduction in operating costs will be investigated.

2. Theory

Dynamic optimization calculates a dynamic trajectory for a control variable (in this case the filtration flux), thus minimizing the operating costs. The operating costs can be divided into: fixed costs, raw feed water costs, pretreatment costs, waste disposal costs and energy costs. Which of these factors predominates depends on the design of the installation and the properties of the feedwater. To compare control modes, the produced volume and the final time are fixed. In that case the only cost factor that can be influenced by variation of the production rate in time is the energy cost.

2.1. Energy consumption

The goal of this study is minimization of energy consumed during the filtration phase. The energy consumption per unit area E, as function of the transmembrane pressure ΔP, the flux J and the pump efficiency η_P is given by:

$$E = \int_0^T \frac{J\Delta P}{\eta_P} \mathrm{d}t \tag{1}$$

At this point a difficulty variable γ is introduced. Conceptually, the difficulty is defined as a normalized ratio between effort and result. Normalization is applied such that the lowest possible value is 1. An increased value indicates how much more effort (power) is needed to obtain the same result (product flow). For membrane filtration, this can be factorized into the difficulty increase due to the pump efficiency (γ_P) and the difficulty increase caused by the fouling resistance (γ_F).

$$\gamma_F = \frac{R}{R_M} \tag{2}$$

$$\gamma_P = \frac{\eta_{P,max}}{\eta_P} \tag{3}$$

in which R_M is the membrane resistance, R the total resistance and $\eta_{P,max}$ is the maximum pump efficiency.

According to Darcy's law, the transmembrane pressure can be given by:

$$\Delta P = \eta R_M J \gamma_F \tag{4}$$

When it is assumed that the viscosity η is constant and Darcy's law is substituted, the energy consumption is given by:

$$E = \frac{\eta}{\eta_{P,max}} R_M \int_0^T \gamma_P \gamma_F J^2 \, \mathrm{d}t \tag{5}$$

The difficulties are described as function of the filtration state and flux by the fouling model and the pump model, respectively.

2.2. Fouling model

Due to the accumulation of retained particles, filtration becomes increasingly more difficult. When it is assumed that there is complete retention and that all retained matter contributes to cake formation, it follows that the change in the fouling state w is equal to the flux:

$$\frac{\mathrm{d}w}{\mathrm{d}t} = J \tag{6}$$

The resistance of an ideal cake R_C depends on the filtration state and the specific cake resistance α [13]:

$$R_C = \alpha w \tag{7}$$

The resistance of a cake inside a hollow fiber is larger than the resistance of the same amount of cake on a flat sheet. A correction factor for this effect is expressed by Φ, which follows from a relationship presented by Belfort et al. [1]:

$$\Phi(w) = -\frac{r}{2wx} \ln\left(1 - \frac{2wx}{r}\right) \tag{8}$$

in which r is the fiber radius and x is the cake volume fraction.

To account for cake compression, the cake resistance is multiplied by another correction factor. This is approximated by a first order function of the uncompressed resistance, $\alpha w\Phi(w)$, the flux, the viscosity and the compressibility β:

$$R_C = \alpha w\Phi(w)(1 + \beta\eta J\alpha w\Phi(w)) \tag{9}$$

Hence, the difficulty caused by the fouling resistance can be given by:

$$\gamma_F(w, J) = 1 + \frac{1}{R_M}\alpha w\Phi(w)(1 + \beta\eta J\alpha w\Phi(w)) \tag{10}$$

2.3. Pump model

The behavior of pumps can be described by their characteristic and efficiency curves. The efficiency curve expresses, for a fixed number of revolutions N, the efficiency $\eta_{P,N}$ as function of the flux J_N. An example of an efficiency curve can be seen in the bottom left corner of Fig. 1. This is approximated by a quadratic function, with $\eta_{P,max}$ the maximum pump efficiency and J_x the flux for which this maximum is attained at the given number of revolutions, it is given by:

$$\eta_{P,N} = \eta_{P,max}\left(1 - \left(\frac{J_N - J_x}{J_x}\right)^2\right) \tag{11}$$

At the same number of revolutions, the relationship between the flow J_N and the head ΔP_N is given by the characteristic curve. This is approximated by a quadratic function, with P_{max} the maximum pressure, it is given by:

$$\Delta P_N = P_{max}\left(1 - \left(\frac{J_N}{2J_x}\right)^2\right) \tag{12}$$

For variable flow pumps, the operating points are not limited to the characteristic curve. To calculate the efficiency for such a point (J, ΔP), the corresponding point on the characteristic curve (J_N, P_N) must be found. The efficiency is constant along certain lines in the J–ΔP plane. A good approximation for such lines can be given by [12]:

$$\Delta P = \frac{\Delta P_N}{J_N^2}J^2 \tag{13}$$

With the help of these equations, the efficiency can be calculated for each combination of flux and pressure. An example can be found in Fig. 1: in the top left graph, the operating point is depicted by O. The corresponding point on the characteristic curve O_N is found by following the line defined by Eq. (13) from the operating point to the characteristic curve. The efficiency at this point follows from the corresponding flow J_N and can be determined from the bottom graph.

By means of the combination of Eqs. (11)–(13) the difficulty due to the pump efficiency can be expressed by:

$$\gamma_P = \left(\frac{\Delta P}{P_{max}}\frac{J_x^2}{J^2} + \frac{1}{4}\right)\left(2\sqrt{\frac{\Delta P}{P_{max}}\frac{J_x^2}{J^2} + \frac{1}{4}} - 1\right)^{-1} \tag{14}$$

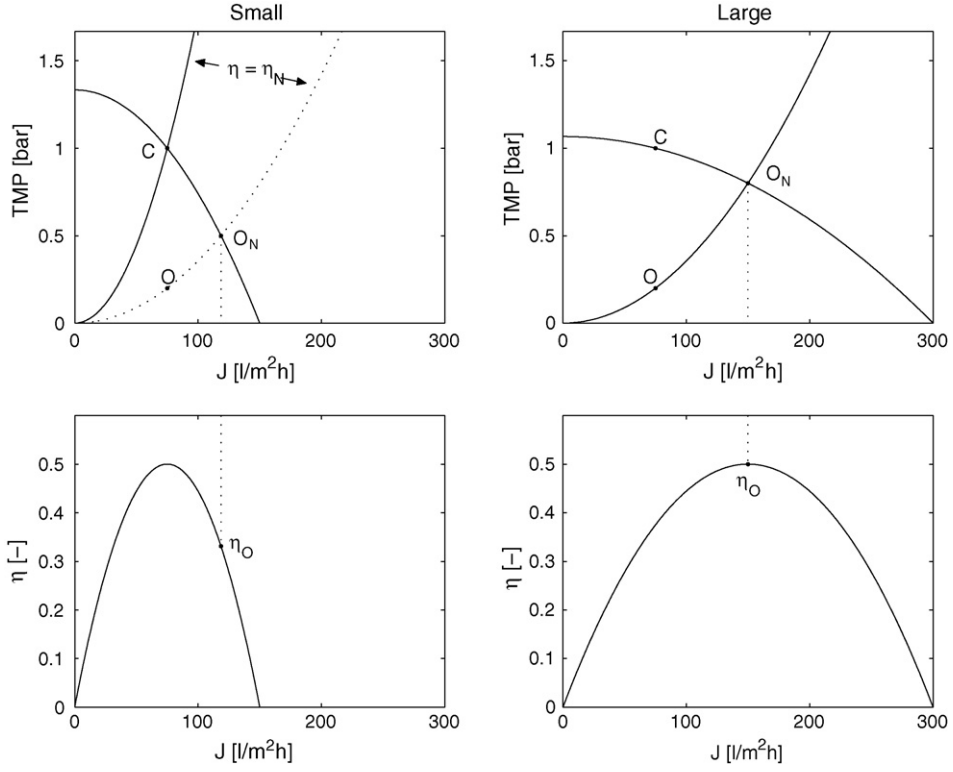

Fig. 1. Characteristic and efficiency curve a small and a large pump. O indicates the operating point, O_N indicates the projection of the operating point on the characteristic curve, C indicates the capacity requirement and η_O indicates the efficiency in the operating point.

2.4. Optimization

The goal of dynamic optimization is to vary the flux over the duration of the filtration phase in such a way that the energy consumption is minimized. The minimum principle can be used to find the optimal trajectory. An introduction to this principle can be found in Ref. [14].

The problem deals with a fixed final time T and final state $w(T) = w_T$, the initial condition is $w(0) = w_0$. The state equation is given by Eq. (6) and the cost functional is given by Eq. (5). Hence, for the system at hand, the Hamiltonian can be defined as

$$\mathcal{H} = \lambda J + \frac{\eta}{\eta_{\mathrm{P,max}}} R_{\mathrm{M}} J^2 \gamma_{\mathrm{P}} \gamma_{\mathrm{F}} \tag{15}$$

The optimal flux minimizes the Hamiltonian. In this case, this means that the derivative of the Hamiltonian with respect to the control variable J must be set to zero.

$$\frac{\partial \mathcal{H}}{\partial J} = \lambda + \frac{\eta}{\eta_{\mathrm{P,max}}} R_{\mathrm{M}} J \gamma_{\mathrm{P}} \gamma_{\mathrm{F}} \left(2 + \frac{J}{\gamma_{\mathrm{P}}} \frac{\partial \gamma_{\mathrm{P}}}{\partial J} + \frac{J}{\gamma_{\mathrm{F}}} \frac{\partial \gamma_{\mathrm{F}}}{\partial J} \right) \tag{16}$$

When this expression is equated to zero and rearranged, it can be substituted in Eq. (15). This gives the value of the Hamiltonian in the optimum:

$$\mathcal{H}^* = - \underbrace{\left(\frac{\eta}{\eta_{\mathrm{P,max}}} J^2 R_{\mathrm{M}} \gamma_{\mathrm{P}} \gamma_{\mathrm{F}} \right)}_{\text{power}} \underbrace{\left(1 + \frac{J}{\gamma_{\mathrm{P}}} \frac{\partial \gamma_{\mathrm{P}}}{\partial J} + \frac{J}{\gamma_{\mathrm{F}}} \frac{\partial \gamma_{\mathrm{F}}}{\partial J} \right)}_{\text{sensitivity for flux}} \tag{17}$$

From optimal control theory it follows that the value of the Hamiltonian is constant, providing no bounds are active. Hence, this equation illustrates the significance of the flux dependency of the difficulty terms. If the difficulty is not sensitive for changes in the flux, it follows directly that constant power operation is optimal.

If the second term increases in time, the power will decrease and vice versa. Hence, when the difficulty does depend on the flux, but the sensitivity does not change in time, constant power is still optimal. Whether it is a good suboptimal strategy, depends on the change of this term along the optimal trajectory.

The optimal control problem is solved numerically, by constructing trajectories with constant Hamiltonian, calculated from Eq. (17).

3. Results

3.1. Parameters

The membrane module, water quality parameters and filtration duration as well as the average flux were chosen based on a pilot plant study. The feedwater used was taken from the Twente Canal and coagulated with polyaluminium chloride. The water quality parameters were determined by filtration at varying flux and composition, as described in Ref. [15].

For comparison, two sets of pump parameters were defined. One maximizes the efficiency in the operating point, while being able to deliver 75 l/m^2 h at 1 bar. This results in a pump with a large flow capacity. The other pump is dimensioned with limited capacity and roughly corresponds to the pilot plant pump. The corresponding characteristic and efficiency curves are shown in Fig. 1. The actual value of the maximum efficiency has no influence on the dynamics of the energy consumption and has therefore no significance for the result. The values of the model parameters are shown in Table 1.

Table 1
Simulation parameters

	Small pump	Large pump
Water quality		
α (m^{-2})	1.00×10^{13}	1.00×10^{13}
β (Pa^{-1})	5.00×10^{-5}	5.00×10^{-5}
x	1.00×10^{-3}	1.00×10^{-3}
η (Pa s)	1.01×10^{-3}	1.01×10^{-3}
Module		
R_{M} (m^{-1})	7.00×10^{11}	7.00×10^{11}
r (m)	4.00×10^{-4}	4.00×10^{-4}
Pump		
P_{max} (Pa)	1.33×10^{5}	1.08×10^{5}
J_{x} (m/s)	4.16×10^{-5}	8.33×10^{-5}
$\eta_{\mathrm{P,max}}$	0.50	0.50
Final conditions		
T (s)	1800	1800
w_0 (m)	0	0
w_T (m)	0.0375	0.0375

3.2. Optimal trajectory

Fig. 2 shows the relative difficulties as a function of the filtration state and the flux. When fouling is considered, it can be seen that due to cake compression it is unfavorable to operate at a high flux when there is a large amount of cake. Hence, it is expected that due to this mechanism the optimum is shifted towards constant pressure filtration. However, when the pump is considered, it can be seen that it is unfavorable to operate at a high flux with little fouling (especially for the small pump) or to operate at a low flux with a large amount of fouling (especially for the large pump). This would shift the optimum towards constant flux filtration.

Figs. 3 and 4 show the resulting trajectories. It can be seen that constant power filtration resembles the optimal trajectory quite well, and is expected to be a good suboptimal strategy.

It can be seen that for the small pump the optimal trajectory is close to constant flux (top left of Fig. 3). For the large pump the optimal trajectory is approximately halfway constant flux and constant pressure (top left of Fig. 4). This is resembles the results that would be obtained for ideal cake filtration [11]. The resemblance with the ideal case is caused by the fact that the pump efficiency shows very little variation and has therefore a small influence on the shape of the filtration trajectory. If the pump would be increased in size even further, the optimal trajectory would shift towards constant pressure filtration.

3.3. Sensitivity

It is interesting to study the effect of model parameters on the optimization results. It should be noted that a very large

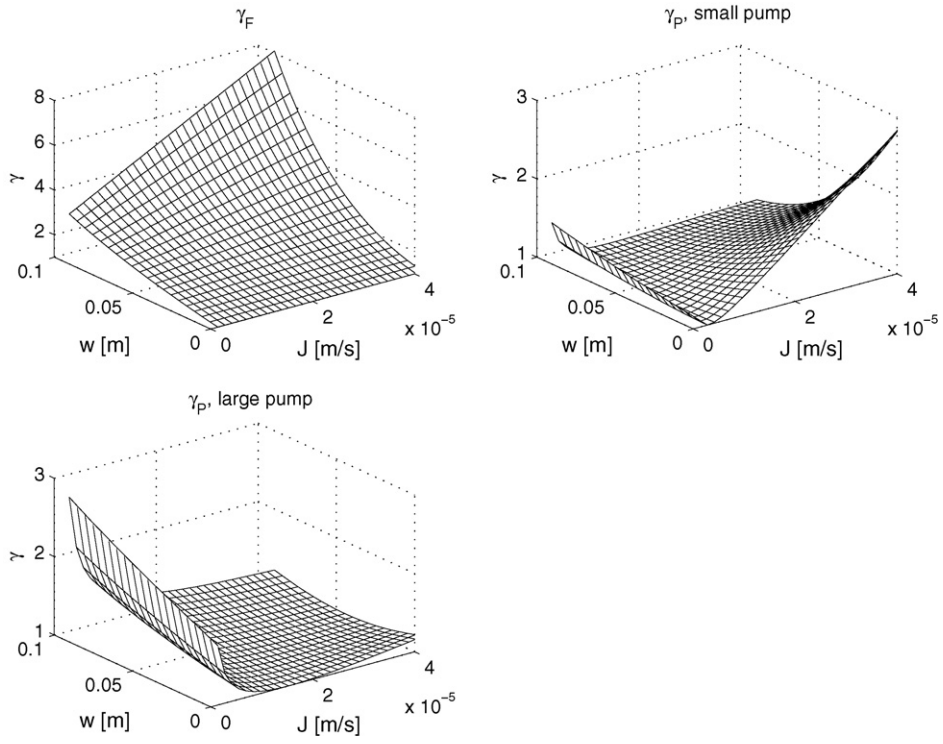

Fig. 2. Top left: difficulty due to fouling; top right: difficulty due to pump efficiency (large pump); bottom: difficulty due to pump efficiency (small pump).

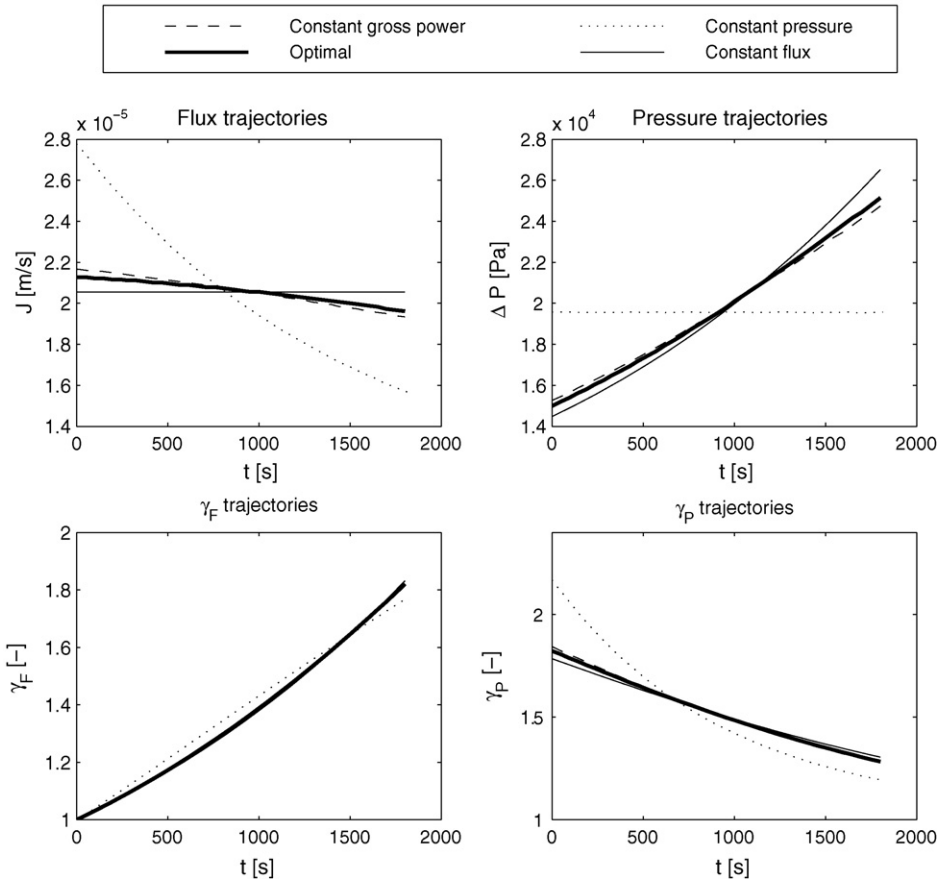

Fig. 3. Flux pressure and difficulty trajectories (small pump).

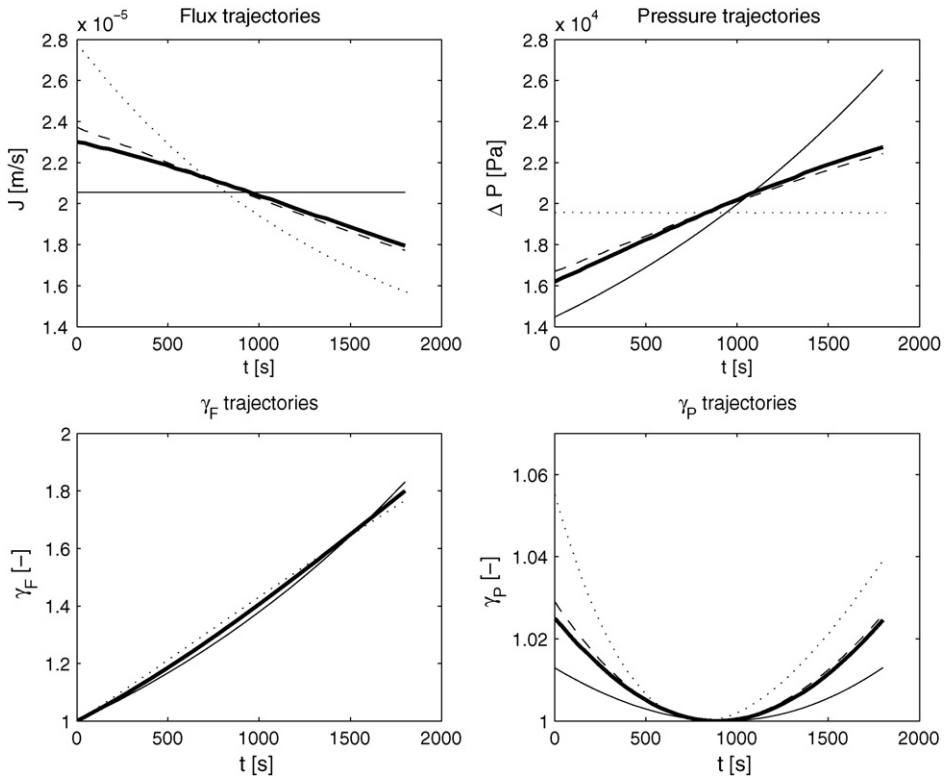

Fig. 4. Flux pressure and difficulty trajectories (large pump).

range of the model parameters will be studied. These values are not necessarily realistic, nor can it be guaranteed the model is accurate in the entire range. The reason for such large varitions is to investigate under which conditions dynamic optimization might be attractive and to illustrate the robustness of suboptimal operating strategies. To compare different situations, two cost indices are defined. The first provides information about how attractive the optimal strategy is compared to reference strategies. The second provides information about the magnitude of the optimal costs under different conditions.

Implementation of a new operating strategy requires adaptation of existing control systems. Whether it is worth this effort, is determined by the difference in the actual energy costs E and the minimal energy costs E^*. To quantify this, the potential savings of a suboptimal strategy are defined as

$$\mathrm{PS} = \frac{E - E^*}{E^*} \tag{18}$$

The value of the potential savings is evaluated under large variations in the model parameters. Thus, it can be estimated under which conditions optimization is attractive.

Some model parameters have a larger effect on the costs and therefore on the operation than others. This is indicated by the relative change in the optimal costs under a certain variation in model parameters. It can be defined as the ratio between the optimal costs for a certain set of parameters E^* and the optimal costs under standard conditions E^*_{ref}.

$$\mathrm{CI}^* = \frac{E^*}{E^*_{\mathrm{ref}}} \tag{19}$$

In the following paragraphs both these values are evaluated and plotted together for several model parameters. Under the investigated conditions, the constant gross power trajectory does not differ significantly from the optimal strategy. Hence, the constant gross power will not appear in the sensitivity plots.

3.3.1. Water quality parameters

The top left of Fig. 5 shows the sensitivity for changes in the specific cake resistance. From the potential savings, as defined by Eq. (18), it can be seen that under normal conditions ($\alpha/\alpha_{\mathrm{ref}} = 1$) the potential savings of the constant flux strategy (line with squares) is not significant (< 0.005 or $< 0.5\%$). However, when the specific cake resistance increases, dynamic optimization becomes more attractive. For example, when the specific cake resistance is 10 times as large as its reference value, approximately 20% more energy is consumed by constant flux filtration than by application of optimal control.

When the cost index, as defined by Eq. (19) (line with triangles), is considered, it can be seen that the optimal costs increase with increasing specific cake resistance. However, when the specific cake resistance is reduced to 10% of its reference value the cost index of the optimal strategy is close to 1. Hence the costs can not be decreased much by reducing the specific cake resistance. This can be explained by the fact that for small α the energy consumption is dominated by the membrane resistance. In that case the different strategies become similar, which is reflected in the relative cost of the suboptimal strategies, which drop below 0.5%.

Fig. 6 shows the same plots for a larger pump. It can be concluded that the optimal costs are more sensitive to changes in

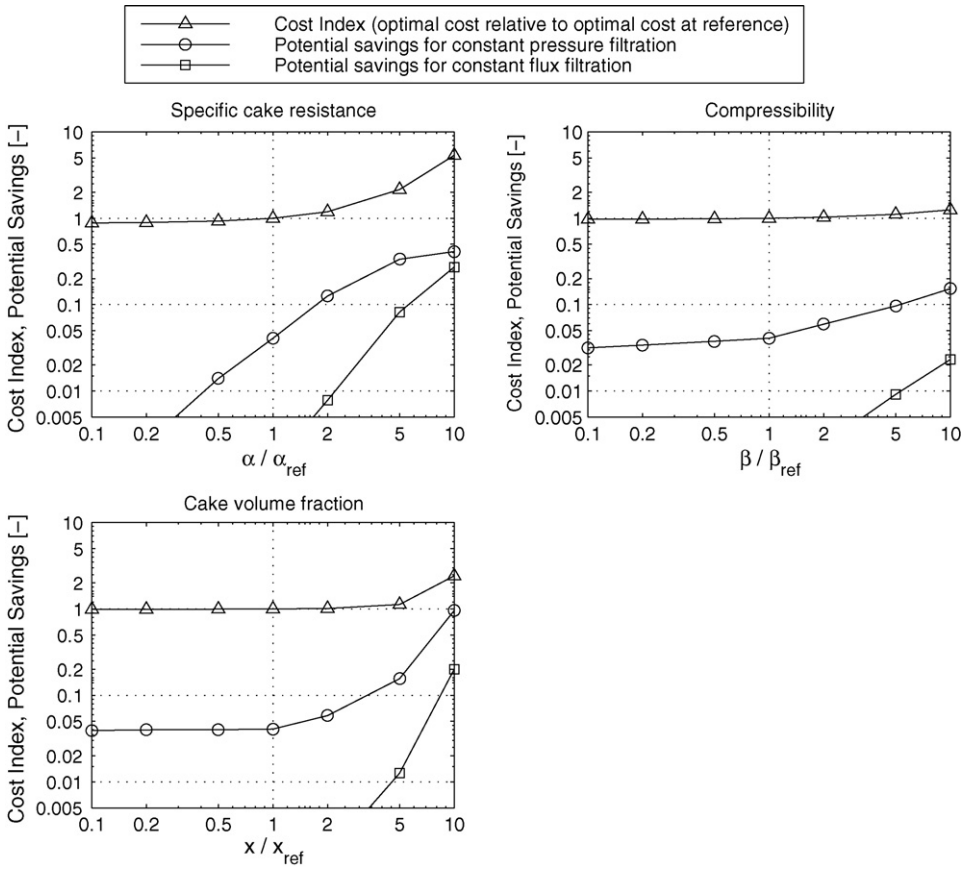

Fig. 5. Effect of water quality parameters on cost index (small pump)

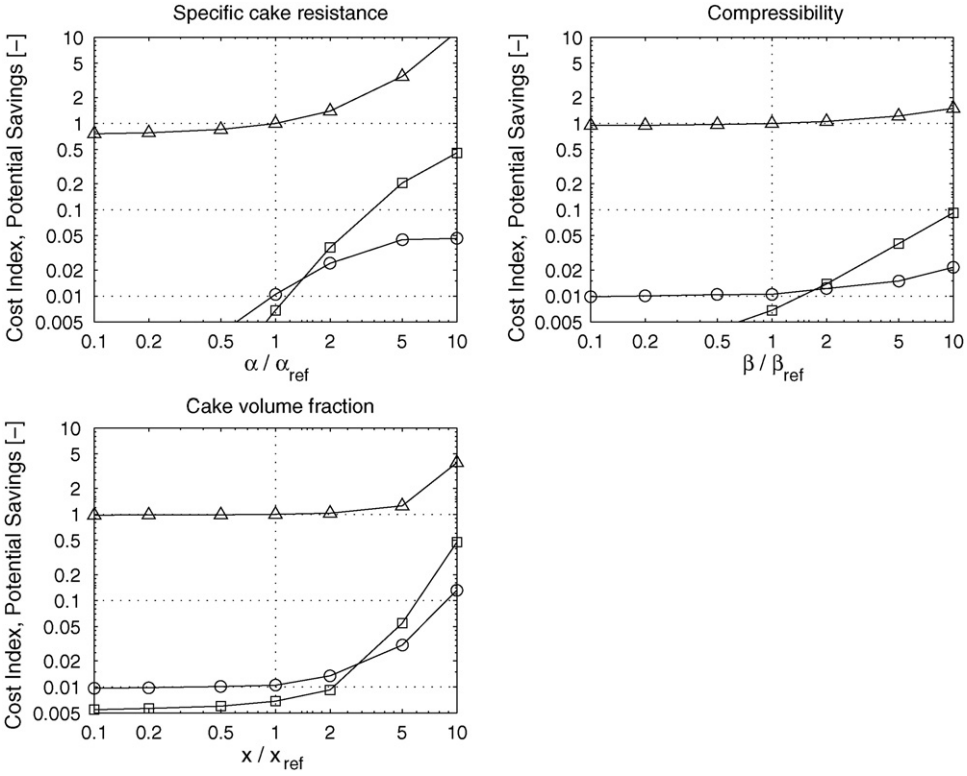

Fig. 6. Effect of water quality parameters on cost index (large pump)

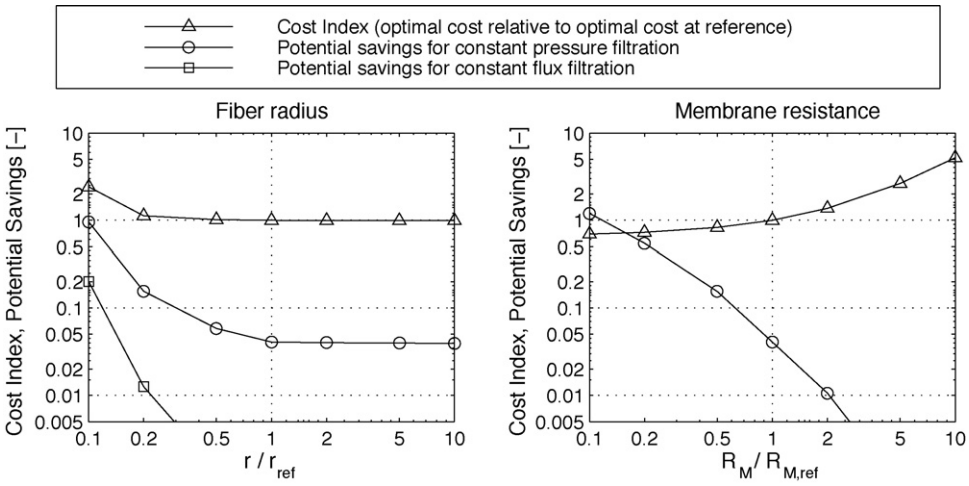

Fig. 7. Effect of module parameters on cost index (small pump)

the specific cake resistance than in the case of the small pump. This can, for example, be seen in the top left plot of Figs. 5 and 6, where an increase of the specific cake resistance to 10 times its reference value leads to an increase of the optimal costs to approximately 5 times its reference value for the small pump, whereas in the case of the large pump the optimal costs are increase by more than a factor 10. This can be explained by the consideration that the efficiency of the small pump improves when the filtration becomes more difficult, because it approaches its operating point. This partially counteracts the effect of changing water quality parameters.

Comparison of the potential savings in both figures, leads to the observation that the relative costs of constant flux filtration is higher for the large pump then for the small pump. This can for

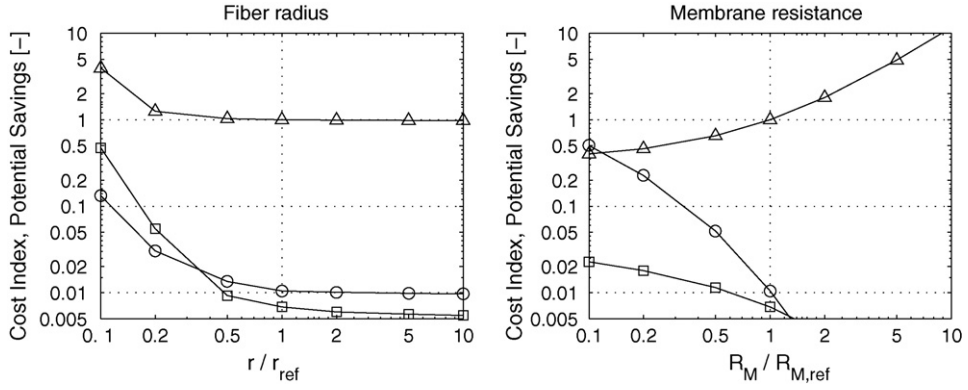

Fig. 8. Effect of module parameters on cost index (large pump)

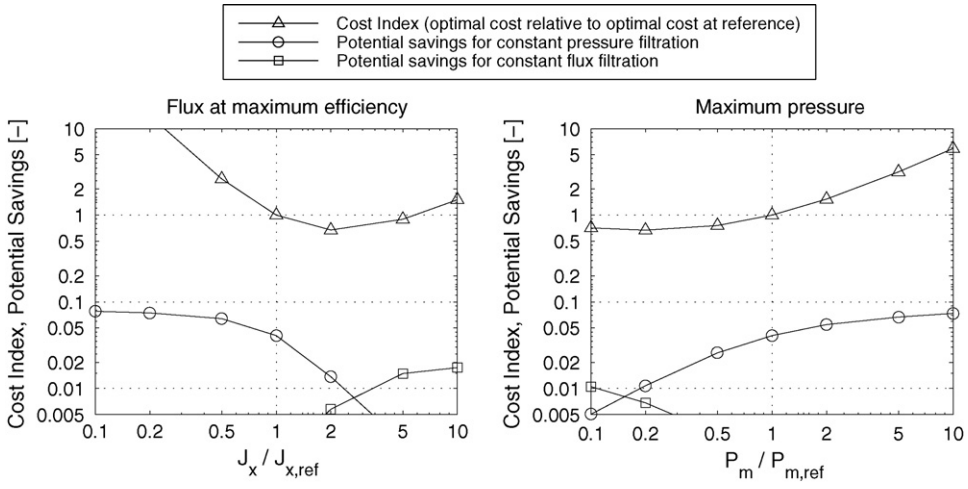

Fig. 9. Effect of pump parameters on cost index (small pump).

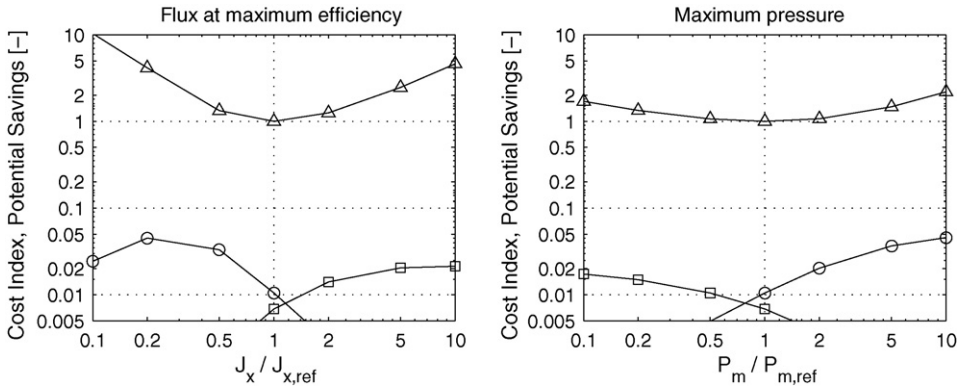

Fig. 10. Effect of pump parameters on cost index (large pump).

example be seen in the top left plots, where going from $\alpha/\alpha_{ref} =$ 1–10 the potential savings of constant flux filtration increase from less than 0.5% to approximately 20% for the small pump and from approximately 0.5% to approximately 50% for the large pump. For constant pressure filtration the opposite effect can be observed.

The compressibility (top right) and the cake volume (bottom left) have only a small influence on the cost, except when these values become large. The potential savings of constant flux and pressure shows that optimization might be attractive when the cake is very compressible or has a very large volume. When realistic values are considered, the viscosity has no significant influence on the potential savings of the reference strategies.

3.3.2. Module parameters

In the right graphs of Figs. 7 and 8 the influence of the membrane resistance on the relative costs is plotted. By lowering the membrane resistance the pump efficiency decreases. This can be seen in Fig. 1, where by lowering the membrane resistance the operating point (O) is shifted down. This reduction in pump efficiency partially countacts the reduc-

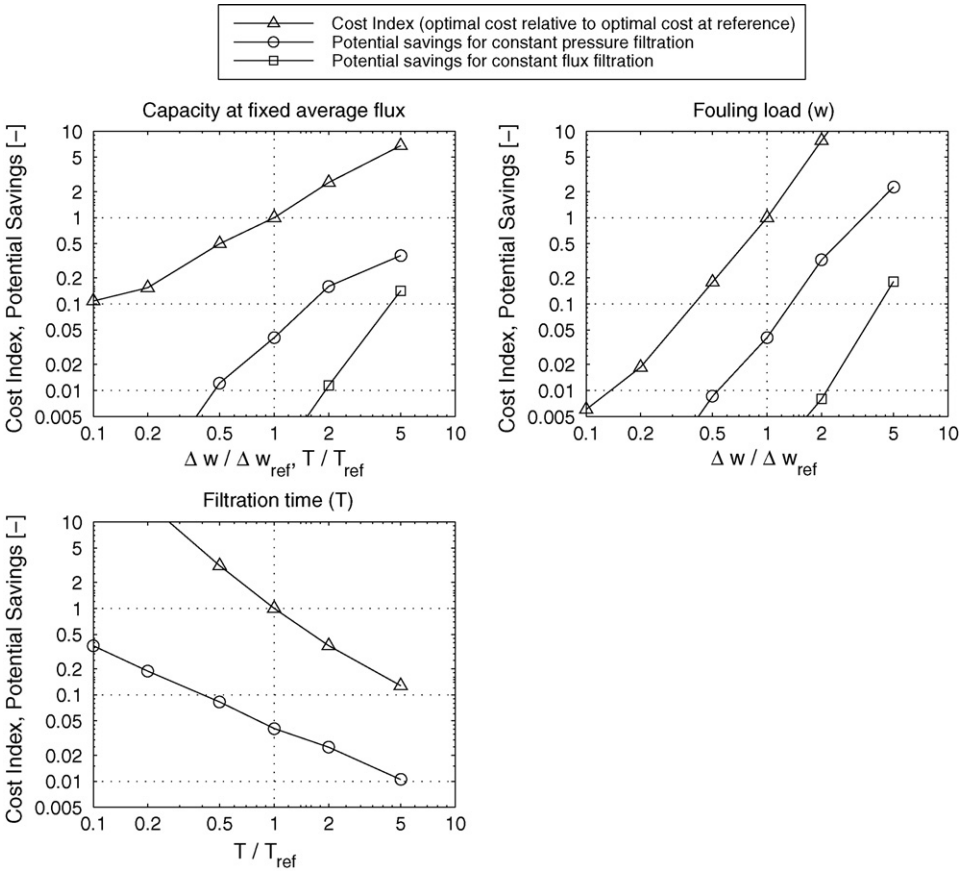

Fig. 11. Effect of final conditions on cost index (small pump).

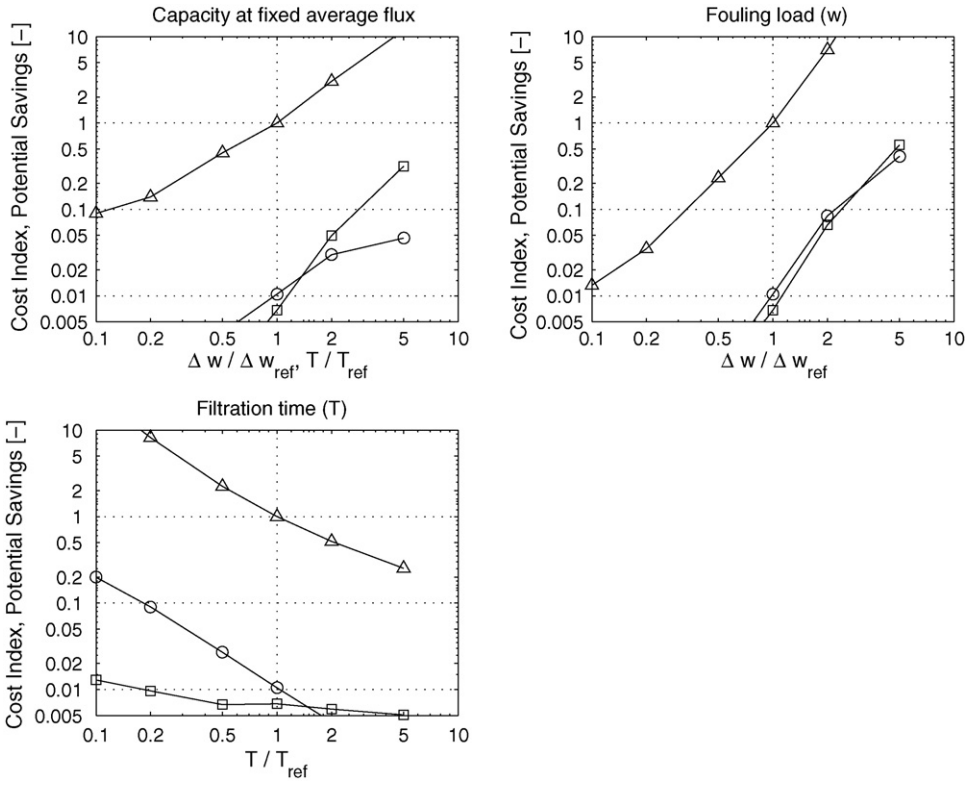

Fig. 12. Effect of final conditions on cost index (large pump).

tion in energy consumption that is expected from lowering the membrane resistance. Furthermore, the change in pump efficiency of the small pump is much larger than the change in efficiency of the large pump. This is reflected in the sensitivity of the optimal costs for changes in the membrane resistance.

When the membrane resistance is lowered, the energy consumption is dominated by the fouling resistance. Consequently, the decrease of the optimal costs that can be achieved by lowering membrane resistance is limited. From the potential savings it can be seen that the optimal strategy becomes more attractive as the membrane resistance gets smaller.

From Eq. (8) it is clear that the effect of the fiber radius is the inverse of the effect of the cake volume fraction. Hence, the left plot of Figs. 7 and 8 are the same as the mirror images of the bottom left plot of Figs. 5 and 6.

3.3.3. Pump parameters

There is a set of pump parameters for which constant flux and constant pressure are (approximately) equally expensive. This is the intersection between the relative costs of constant pressure and constant flux filtration. This point can be seen in Figs. 9 and 10. If, compared to this point, the the pump has a large head P_m and/or a small capacity J_x, constant pressure is more expensive than constant flux and vise versa. Since this intersection is close to the reference for the large pump, it can be concluded that unless the pump is over dimensioned, constant flux filtration will typically consume less energy than constant pressure filtration.

3.3.4. Final conditions

Figs. 11 and 12 show the sensitivities of the costs towards changes in the final conditions. Three possibilities of changing the final conditions are considered, which are:

(1) Variable final state and final time at a fixed ratio. In this case the filtration duration is varied, while maintaining the same average production rate. As can be seen in the top left graph of Figs. 11 and 12 the optimal costs vary approximately linearly with the fouling load.
(2) Variable final time and fixed final state. When the same volume is produced in less time, the average flux increases, whereas the amount of fouling remains the same. In Eq. (1) it can be seen that the energy costs are approximately proportional to the square of the average flux.
(3) Variable final state and fixed final time. When more is produced in the same time, both the average flux and the amount of fouling increase. Since both effects occur, the optimal costs are approximately proportional to the third power of the fouling load.

Furthermore, it can be seen that optimization becomes more attractive when the fouling load gets larger and/or the average flux increases.

4. Conclusion

Constant flux filtration consumes less energy than constant pressure filtration. This difference can be mainly accounted to

the pump efficiency, which is determined by the pump dimensions. For pumps with equal head but a larger capacity, the optimum shifts towards constant pressure filtration. Under typical conditions, the potential savings of constant flux and constant gross power compared to the optimal strategy are small (<1%). When the fouling load and production rate increase, the difference between the operating strategies becomes more significant. However, for industrial applications the advantage of a constant production rate achieved in constant flux filtration probably outweighs the energy that can be saved by applying constant gross power filtration.

Acknowledgements

The financial support by: NWO/STW, Aquacare Europe, Hatenboer-Water, Norit Membrane Technology and Vitens Lab & Procestechnology is gratefully acknowledged.

Nomenclature

E	energy consumption (J/m^2)
E^*_{ref}	optimal energy consumption at standard conditions (J/m^2)
$\mathcal{H}$	hamiltonian (W/m^2)
J	flux (m/s)
J_{N}	flux (in characteristic curve) (m/s)
J_{x}	flux with maximum efficiency in charcteristic curve (m/s)
$\mathcal{J}$	goal functional (J/m^2)
P	power (W/m^2)
$P_{\max}$	maximum pressure (Pa)
ΔP	transmembrane pressure (Pa)
ΔP_{N}	transmembrane pressure (in characteristic curve) (Pa)
r	fiber radius (m)
R	resistance (m^{-1})
R_{C}	cake resistance (m^{-1})
R_{M}	membrane resistance (m^{-1})
t	time (s)
T	final time (s)
T	temperature (°C)
w	fouling state (m)
x	cake volume fraction

Greek letters

α	specific cake resistance (m^{-2})
β	compressibility (Pa^{-1})
γ_{P}	'difficulty' due to pump efficiency
γ_{F}	'difficulty' due to fouling
η	viscosity (Pa s)
η_{P}	pump efficiency
$\eta_{\text{P,N}}$	pump efficiency (in characteristic curve)
$\eta_{\text{P,max}}$	maximum pump efficiency
λ	adjoined state (Pa)
Φ	volume correction factor

Indices

0	initial ($t = 0$)
T	final ($t = T$)
*	optimal

References

[1] G. Belfort, R.H. Davis, A.L. Zydney, The behavior of suspensions and macromolecular solutions in crossflow microfiltration, J. Membr. Sci. 96 (1994) 1–58.
[2] Y. Xu, J. Dodds, D. Leclerc, Optimization of a discontinuous microfiltration-backwash process, Chem. Eng. J. 57 (1995) 247–251.
[3] W.D. Mores, C.N. Bowman, R.H. Davis, Theoretical and experimental flux maximization by optimization of backpulsing, J. Membr. Sci. 165 (2000) 225–236.
[4] M. Noronha, V. Mavrov, H. Chmiel, Simulation model for optimisation of two-stage membrane filtration plants-minimising the specific costs of power consumption, J. Membr. Sci. 202 (2002) 217–232.
[5] A.J.B. van Boxtel, Z.E.H. Otten, H.J.L.J. van der Linden, Dynamic optimization of a one-stage reverse osmosis installation with respect to membrane fouling, J. Membr. Sci. 65 (1992) 277–293.
[6] M. Decloux, L. Tatoud, Importance of the control mode in ultrafiltration: case of raw cane sugar remelt, J. Food Eng. 44 (2000) 119–126.
[7] H. Carrère, F. Blaszkow, Comparison of operating modes for clarifying lactic acid fermentation broths by batch cross-flow microfiltration, Process Biochem. 36 (2001) 751–756.
[8] H. Carrère, F. Blaszkowa, H. Roux de Balmann, Modelling the microfiltration of lactic acid fermentation broths and comparison of operating modes, Desalination 145 (2002) 201–206.
[9] C. Ho, A.L. Zydney, Transmembrane pressure profiles during constant flux microfiltration of bovine serum albumin, J. Membr. Sci. 209 (2002) 363–377.
[10] S. Chellam, W. Xu, Blocking laws analysis of dead-end constant flux microfiltration of compressible cakes, J. Colloid Interf. Sci. 301 (2006) 248–257.
[11] B. Blankert, B.H.L. Betlem, B. Roffel, Dynamic optimization of a dead-end filtration trajectory: blocking filtration laws, J. Membr. Sci. 285 (2006) 90–95.
[12] I.J. Karassik, W.C. Krutzsch, W.H. Fraser, J.P. Messina, Pump Handbook, McGraw-Hill Inc., 1976.
[13] J. Hermia, Constant pressure blocking filtration laws—application to power-law non-newtonian fluids, Trans. IChemE 60 (1982) 183–187.
[14] W.F. Ramirez, Process Control and Identification, Academic Press, Boston, 1994.
[15] H. Futselaar, B. Blankert, B.H.L. Betlem, M. Wessling, Method for monitoring the degree of fouling of a filter, Int. Patent WO2006031099.